Influence of ligand groups in Ti precursors on phase transformation and microstructural evolution of TiO_2 thin films prepared by the wet chemical process

Chu-Chi Ting and San-Yuan Chen[a)]
Department of Materials Science and Engineering, National Chiao-Tung University, Hsinchu, Taiwan 300, Republic of China

(Received 5 June 2000; accepted 23 March 2001)

TiO_2 thin films prepared by metalorganic decomposition (MOD-TiO_2) and sol-gel processes (SG-TiO_2) were investigated in terms of the anatase-to-rutile phase transformation and microstructural evolution. It was found that the chemical reactivity of the ligand groups initially coordinated on the titanium precursor plays a decisive role in the structure development of as-deposited SG- and MOD-TiO_2 films. MOD-TiO_2 films consist of small aggregated particles and therefore, tend to coalesce together to form an inhomogeneous microstructure during the anatase-to-rutile phase transformation. On the other hand, SG-TiO_2 films consist of uniform large particles that tend to grow homogeneously. MOD-TiO_2 films showed a higher crystallization temperature than the SG-TiO_2 films but the temperature of the anatase-to-rutile phase transformation is much lower in MOD- (approximately 775 °C) as compared to SG-TiO_2 films (approximately 930 °C). The activation energy (Q) was estimated as 524 and 882 kJ/mol for the MOD- and SG-TiO_2 films, respectively. The lower transformation temperature and activation energy in MOD-TiO_2 films were due to smaller grain size and more potential nucleation sites existing in the un-transformed MOD-TiO_2 film structure, which can accelerate the rate of anatase-to-rutile transformation.

I. INTRODUCTION

Titanium dioxide thin films have received great attention in recent years because of their excellent optical and electronic properties.[1–3] The wet chemical route, including metalorganic deposition (MOD) and sol-gel methods, has been recognized to be technologically and economically significant because they offer advantages over conventional techniques such as relatively low processing temperatures. In the sol-gel process, metal alkoxides $Ti(OR)_4$ (where R represents alkyl groups) are generally used as principal precursors. Further hydrolysis and polymerization cause the formation of a three-dimensional network structure with octahedral TiO_6 coordination.[4–8] In contrast to the sol-gel method, the MOD process typically employs metal carboxylate precursors with long carbon chains such as titanium 2-ethylhexoxide, which is chemically stable and insensitive to water molecules. Polymerization of the MOD precursors seems inaccessible, and the formation of a three-dimensional network structure is impossible. The coordination number of the Ti atom is maintained at 4 in the MOD solution. Therefore, from a comparative viewpoint, the nature of ligand groups in titanium precursors should affect the final structure of the crystalline TiO_2 to a certain extent.

The TiO_2 crystal has three modification phases, namely, anatase, rutile, and brookite; however, only the first two have received most attention. The rutile phase is a high-temperature stable phase (>700 °C), while the anatase is stable only at lower temperature.[9,10] Both crystalline phases are composed of octahedral TiO_6 where one Ti atom is coordinated with 6 oxygen atoms. The phase transformation of anatase-to-rutile (A $\rightarrow$ R) in TiO_2 is a research objective of considerable interest with respect to both powder and thin film. Even though the A $\rightarrow$ R phase transformation of TiO_2 powder derived from the hydrolysis of titanium alkoxides has been studied, many earlier works are mainly focused on the influence of hydrolysis kinetics.[11–13] Furthermore, the lower-dimensional configuration of the thin-film form usually gives rise to an enhanced complexity in the phase transformation (and kinetics as well) by the constraint induced by the underlying substrate.[14] Literature reports of the influence of the ligand group on the phase transformation as well as the microstructural evolution in the synthesis of TiO_2 thin films are not extensive.

[a)]Address all correspondence to this author.
e-mail: sychen@cc.nctu.edu.tw

Therefore, we conducted a comparative study between sol-gel and MOD processes using Ti precursors with a significant difference in ligand nature. Both films were subjected to an identical heat treatment. We wish to understand (i) how the coordinated ligand groups affect the A $\rightarrow$ R phase transformation, (ii) the microstructural evolution, and (iii) the activation energy of the A $\rightarrow$ R phase transformation for the sol-gel and MOD-TiO_2 films.

II. EXPERIMENTAL PROCEDURE

A. Sol-gel and MOD solution preparation

Titanium isopropoxide $Ti(OC_3H_7^i)_4$ (Alfa, 99.8%) was used as a titanium precursor in the sol-gel process. The reactivity of titanium isopropoxide toward water is first modified by acetic acid (TEDA, 99.9%) (molar ratio of Ti/HOAc = 1/10). Then 2-methoxyethanol (Merck, 99%) (Darmstadt, Germany) was added to adjust the viscosity and molar concentration of the mixture. The methoxyethanol not only acts as solvent but also reacts with unreacted acetic acid to form isopropyl acetate and water. This sol-gel solution with titanium molar concentration of approximately 0.47 M was vigorously stirred at room temperature for 10 h to ensure a sufficient degree of hydrolysis and polycondensation.

Titanium 2-ethylhexoxide $Ti(C_8H_{17}O)_4$ (Alfa, 98%) was used as a titanium precursor in the MOD process. P-xylene was used as a solvent to reduce the viscosity of the titanium 2-ethylhexoxide for film fabrication. The molar concentration of titanium ions in MOD solution was about 0.93 M.

B. Fabrication of thin films

The thin films were fabricated by spin coating onto fused silica substrates at a rotation speed of 3000 rpm for 30 s. After each deposition, the coating film was dried on a hot plate (approximately 200 °C for 2 min) to remove the organic solvent and then pyrolyzed in air at 400 °C for 10 min with a heating rate of 5 °C/min to decompose organic species. For multiple coatings, the above-mentioned processes were repeated six times to obtain the resulting sol-gel and MOD-TiO_2 films with a thickness of approximately 300 nm. For a phase transformation study, the resulting films were directly annealed into a preheated furnace with temperatures between 500 and 1000 °C under an air environment for various time periods.

C. Film characterization

The phase evolution of sol-gel and MOD films was examined by an x-ray diffractometer (MAC Science, M18X) (Tokyo, Japan) using Cu K_α radiation. The thickness of the films was measured using a surface profiler (Sloan, Dektak^{3}ST). The xerogel powder scraped from the dried film on the substrate was mixed with KBr and then was die pressed to be a pellet for the Fourier transform infrared (FTIR) transmission spectra measurement (with Perkin-Elmer 580 spectrometer). The microstructure of the films was examined using scanning electron microscopy (SEM; Hitachi, S4000) (Tokyo, Japan). The average grain size in the TiO_2 films after different annealing temperatures was estimated using linear intercepts on the SEM micrographs according to the technique developed by Mendelson *et al.*[15]

III. RESULTS AND DISCUSSION

A. Role of titanium precursors in phase evolution

Figure 1 shows the XRD patterns of the sol-gel-derived TiO_2 films (designated as SG-TiO_2). Crystalline anatase first appeared with a weak (101) peak at 400 °C. However, no rutile phase was detectable until a temperature as high as 930 °C was attained where a characteristic reflection of the (110) peak appeared. It is interesting to note that the transformation temperature for the SG-TiO_2 film is higher by approximately 300 °C than that of nanocrystalline TiO_2 powders, 650–700 °C and sputtered TiO_2 films, approximately 700 °C.[16,17] On the other hand, an anatase phase with a strong (101) reflection appeared when the temperature reached 500 °C for the MOD-TiO_2 films, as shown in Fig. 2. The formation temperature of rutile phase is about 750–775 °C, which is lower by approximately 200 °C than that observed for SG-TiO_2 films, and is only higher by approximately 50 °C than temperatures reported for the nano-powder TiO_2.[16] If we refer to this additional 50 °C as a corresponding extra energy required to overcome the substrate

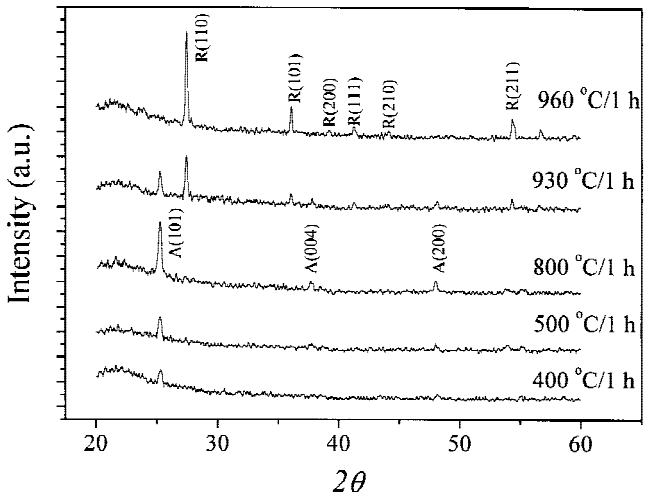

FIG. 1. XRD patterns of SG–TiO_2 films annealed at different temperatures for 1 h.

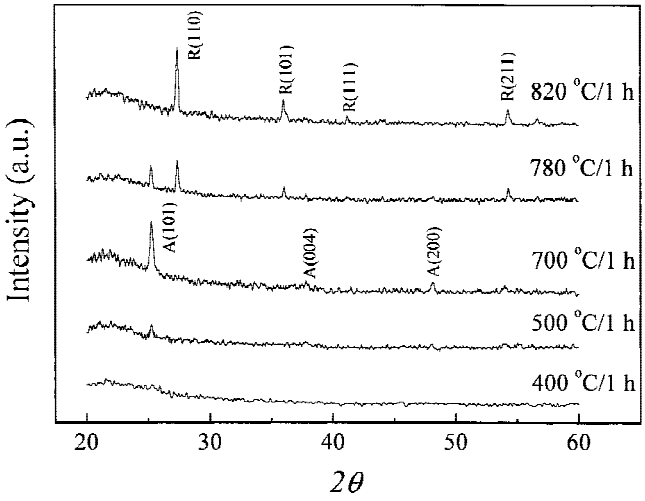

FIG. 2. XRD patterns of MOD-TiO_2 films annealed at different temperatures for 1 h.

constraint, then, on a comparative basis, more energy (i.e., the additional 250 °C increment) is required to trigger the phase transformation in the SG-TiO_2 films.

Since the only variable in the preparation of both films is the difference in the starting chemical precursors, this leads us to suggest a possible cause resulting from the difference in chemical reactivity between $Ti(OC_3H_7^i)_4$ and $Ti(C_8H_{17}O)_4$. For the sol-gel process, the titanium isopropoxide can be first modified by acetic acid to produce titanium isopropoxide acetate, which undergoes further hydrolysis and polycondensation to form a three-dimensional TiO_6 network structure.[4–6,18]

The IR transmission spectrum of the dried SG-TiO_2 film is analyzed and shown in Fig. 3. The broad band around 3500 cm^{-1} is due to O–H stretching vibrations

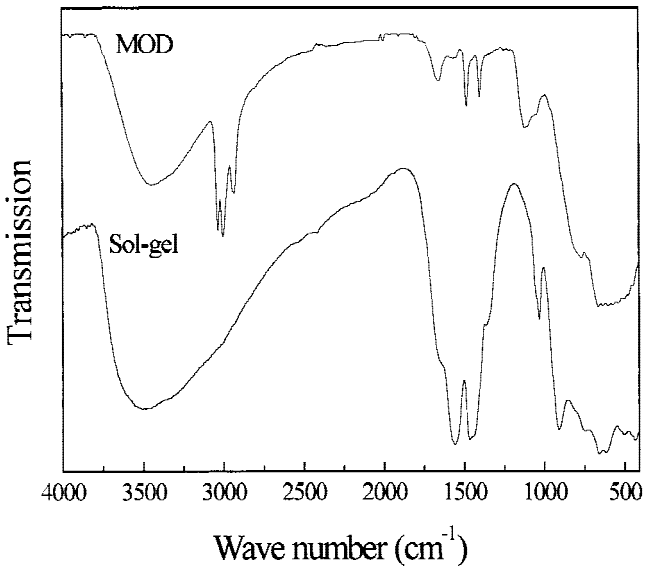

FIG. 3. FTIR transmission spectra of dried SG- and MOD-TiO_2 films.

of the hydroxyls present in the system. Two bands assigned as υ_{sym}(COO) at 1455 cm^{-1} and υ_{asym}(COO) at 1560 cm^{-1} are consistent with those defined as bidentate ligands.[19–21] Compared with the FTIR spectrum of titanium isopropoxide, the bands around 2960–2870 cm^{-1} corresponding to the stretching vibrations of the CH_2 and CH_3 in isopropoxy ligands does not appear.[5,22] In addition, the band around 1030 cm^{-1} due to the Ti(O–C) stretching vibration of the isopropoxy groups bonded to titanium ions obviously weakened,[5,22,23] implying the displacement of isopropoxy groups from titanium ions. The bands between 800 and 400 cm^{-1} could be attributed to Ti–O–Ti bonds.[5,22,24,25] Thus, these observations indicate that titanium isopropoxide moleculars have undergone hydrolysis/polymerization reaction and formed a three-dimensional network structure.

In contrast, the IR spectrum of the dried MOD-TiO_2 film exhibits sharp bands around 2960–2870 cm^{-1} and 1475–1395 cm^{-1} corresponding to the stretching and bonding vibrations of the CH_2 and CH_3 groups in 2-ethylhexoxy ligands, respectively. The bands around 1200–1000 cm^{-1} can be assigned as a result of stretching mode of Ti(O–C), indicating that Ti atoms still coordinated with 2-ethylhexoxy groups. As expected, no Ti–O–Ti bond was detected, suggesting that Ti atoms are still tetra-coordinated with four 2-ethylhexoxy ligands (i.e., titanium 2-ethylhexoxide did not undergo hydrolysis/condensation reaction, so the as-deposited MOD-TiO_2 film still consists of titanium 2-ethylhexoxide monomers).

B. Phase crystallization and transformation

Comparing Figs. 1 and 2 shows that a lower crystallization temperature (T_{cry}) is obtained for the SG-TiO_2 (T_{cry} = approximately 400 °C) than the MOD-TiO_2 (T_{cry} = approximately 500 °C) films. This phenomenon indicates that the chemical reactivity of the ligand groups initially coordinated with the Ti atom plays a decisive role in the subsequent crystallization process. When the as-deposited MOD-TiO_2 film is pyrolyzed from room temperature to 400 °C, more energy must be consumed to break the organic bonds of titanium 2-ethylhexoxide monomers. Subsequently, both Ti and O atoms rearrange themselves to form a three-dimension network structure. On the other hand, since a disorder three-dimensional network structure has already formed in the as-deposited SG-TiO_2 films, the less energy is required for the re-arrangement of the disorder structure to form a long-range order octahedral TiO_6 network structure. Consequently, the anatase phase can be crystallized at a lower temperature for the SG- than MOD-TiO_2 films.

In addition, an appreciable difference in the temperature (T_{tran}) for the A → R phase transformation was observed (i.e., T_{tran} = 750 to 770 °C for the MOD-TiO_2

film and T_{tran} = 900 to 930 °C for the SG-TiO_2 films, reflecting to a relatively higher energy for the SG-TiO_2 films to initiate the A → R phase transformation than that for the MOD-TiO_2 films). However, this finding is opposite to that observed for the crystallization temperature mentioned above. This can be attributed to the fact that the as-pyrolyzed SG-TiO_2 film (i.e., the film was heat-treated at 400 °C for 1 h) has a better crystallinity (i.e., less lattice defects) than as-pyrolyzed MOD-TiO_2 film.

The role of oxygen defects (vacancies) in the A → R phase transformation has been most-commonly reported.[10,26,27] Shannon *et al.*[10] introduced oxygen vacancies into TiO_2 crystals by using a hydrogen atmosphere. They believed that the oxygen vacancies promote the Ti–O bond rearrangement, which in turn enhances the A → R phase transformation rate. Their explanation may be applicable to the transformation currently observed. However, in addition to oxygen defects, the difference in the rate of phase transformation between the SG- and MOD-TiO_2 films is also strongly related to grain size.[16] This is further elucidated in terms of the microstrutural evolution in the forthcoming discussion.

To understand the difference of A → R phase transformations between the SG- and MOD-TiO_2 films, we estimate the phase variation using the following equation.[16,28] Although this equation is based on the A → R phase transformation of titania powder, it is also adopted in our films because the x-ray diffraction (XRD) patterns of polycrystalline anatase/rutile phase in SG- and MOD-films are similar to those of powdered samples with completely random crystal orientations. The transformed fraction of rutile phase (y) is defined as Equation (1),

$$y = \frac{1}{\left[1 + 0.8 \times \frac{I_A}{I_R}\right]} \quad , \qquad (1)$$

where I_A/I_R represent the x-ray integrated intensity ratio of the (101) reflection of the anatase and the (110) reflection of the rutile. The resulting y is plotted in terms of annealing time (t) for both films. The relationship is shown in Figs. 4(a) and 4(b) where both films show a similar y-time sigmoidal curve for different annealing temperatures. In addition, there exists an annealing time period after which a measurable formation amount of rutile phase can be detected by XRD. The period is termed the incubation time and also related to precursor used. The pronounced sigmoidal relationship still signifies a nucleation-growth mechanism of the phase transformation that is consistent with previous observation on powdered TiO_2 irrespective of factors such as the constraint effect induced by the underlying substrate and the presence of an amorphous component (those two factors can cause a change in the rate of phase transformation).[10,29]

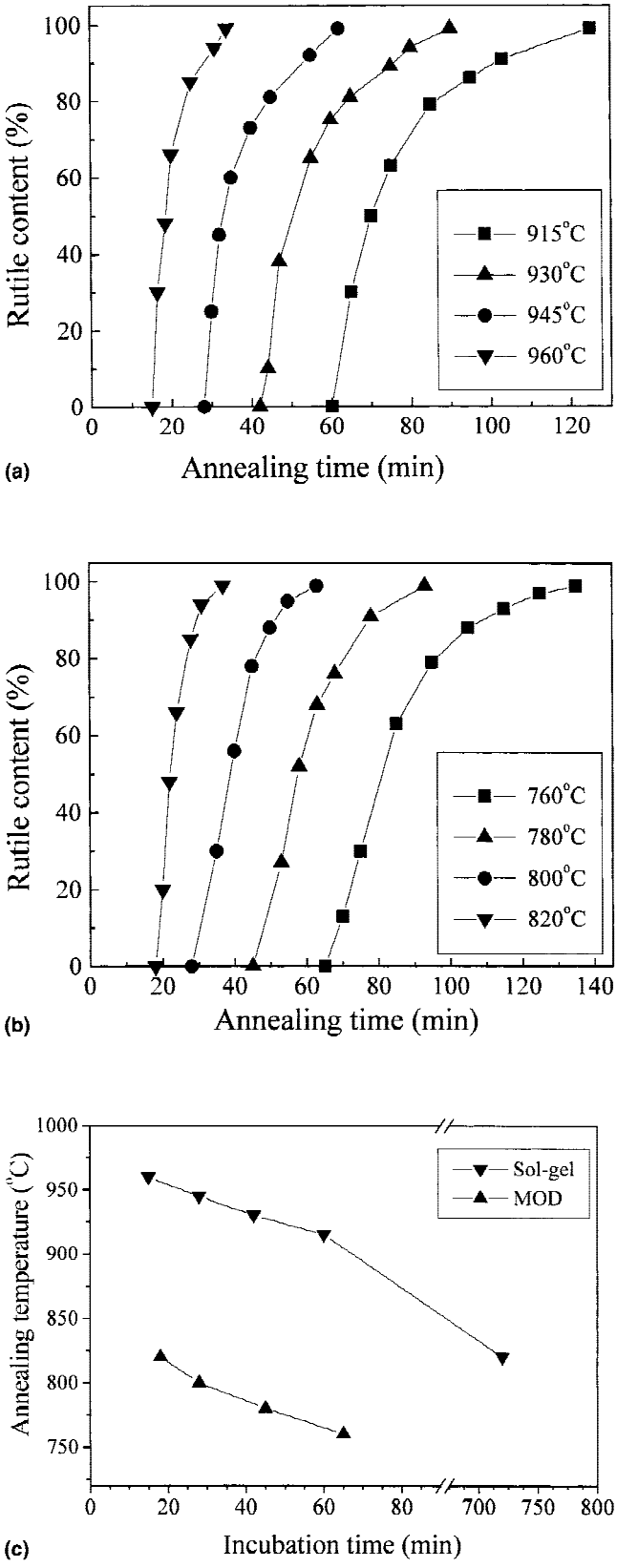

FIG. 4. The transformed fraction of rutile phase for (a) SG-TiO_2 and (b) MOD-TiO_2 films under different annealing temperatures and time in air. (c) Incubation time as a function of annealing temperatures for the anatase to rutile phase transformation.

The incubation time of SG- or MOD-TiO_2 films is much longer than that of powdered TiO_2.[10] This phenomenon can be attributed not only to the substrate constraint effect, but also to the amorphous-to-anatase (Am $\rightarrow$ A) transformation. Namely, the amorphous phase seems to first transform to an anatase phase, and then the anatase phase transforms to rutile. Furthermore, the MOD-TiO_2 films have much shorter incubation time, as compared to the SG-TiO_2 films under identical annealing temperature [see Fig. 4(c)], indicating that a faster rate of nucleation and/or growth can be achieved for the MOD-TiO_2 film.

C. Microstructural evolution

The A $\rightarrow$ R phase transformation is a nucleation-growth process. Shannon *et al.*[30] reported that the crystallography of the transformation using anatase TiO_2 single crystals showed that the rutile phase was nucleated on the surface and then spread into to the anatase TiO_2. The surface or grain boundaries nucleation in the nanocrystalline anatase TiO_2 for A $\rightarrow$ R phase transformation was also observed by Kumar *et al.*[31] and Ding *et al.*[16] Gribb *et al.*[32] demonstrated that the rate of the polymorphic anatase to rutile transformation increases dramatically when the reacting anatase is very finely crystalline. Namely, the smaller anatase crystallite size possesses the more number of potential nucleation sites. So the rate of A $\rightarrow$ R phase transformation will be accelerated. Therefore, it is believed that the SG- and MOD-TO_2 films synthesized from different titanium precursors should possess different numbers of potential nucleation sites, which can cause the obvious differences in A $\rightarrow$ R phase transformation between the SG- and MOD-TiO_2 films. The distinct evolution of microstructural morphology might provide clues for a better understanding of the observed phase transformation.

The SG-TiO_2 film exhibits a dense microstructure with an average grain size of approximately 35 nm at 700 °C, Fig. 5(a). The grains grew uniformly from 49 to 127 nm with increased annealing time at 930 °C, as shown in Figs. 5(b)–5(d). For the MOD-TiO_2 film at 700 °C, a surface morphology similar to that of SG-TiO_2 [Fig. 5(a)] is observed, but the grain size is smaller, i.e., approximately 27 nm, as shown in Fig. 6(a). However, a porous structure with a number of aggregated grains developed when the annealing temperature/time was increased to 780 °C/30 min [Fig. 6(b)], a temperature at which the phase transformation had not occurred. Further increase in annealing time causes aggregated grains to coalesce to form larger grains, as indicated by the arrows in Fig. 6(c), and an exaggerated grain growth was later observed, resulting in a bimodal grain size distribution [Fig. 6(d)].

As expected from the phase transformation aforementioned, both films show an essentially different behavior of microstructural evolution. Because the number of potential nucleation sites is proportional to the specific surface area (SSA) of a crystalline grain, the number of potential nucleation sites will increase with decreasing grain size. Consequently, the transformation rate will be accelerated. In other words, the difference of the SSA

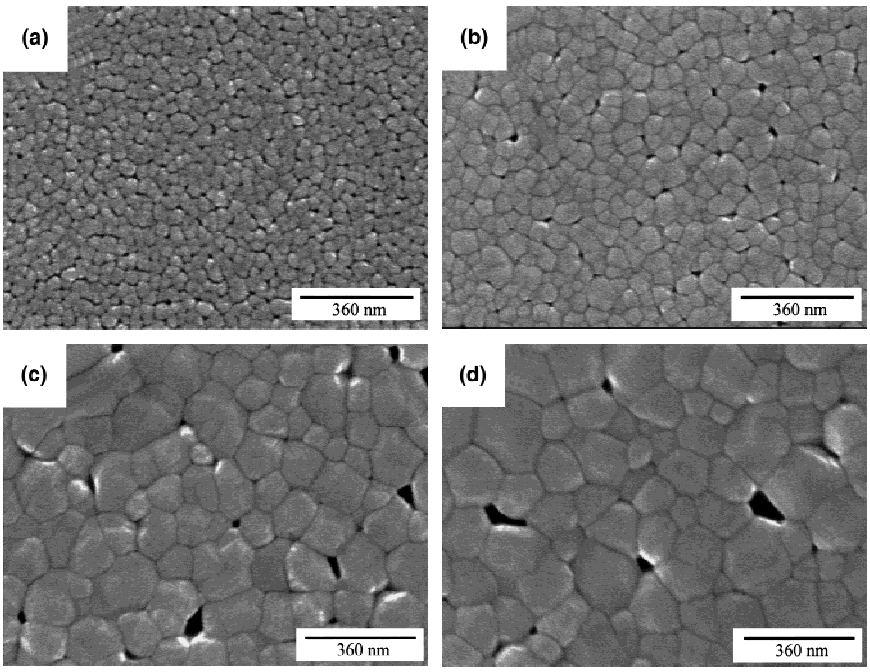

FIG. 5. Microstructural evolution of SG-TiO_2 films annealed at (a) 700 °C/60 min, (b) 930 °C/30 min, (c) 930 °C/60 min, and (d) 930 °C/90 min.

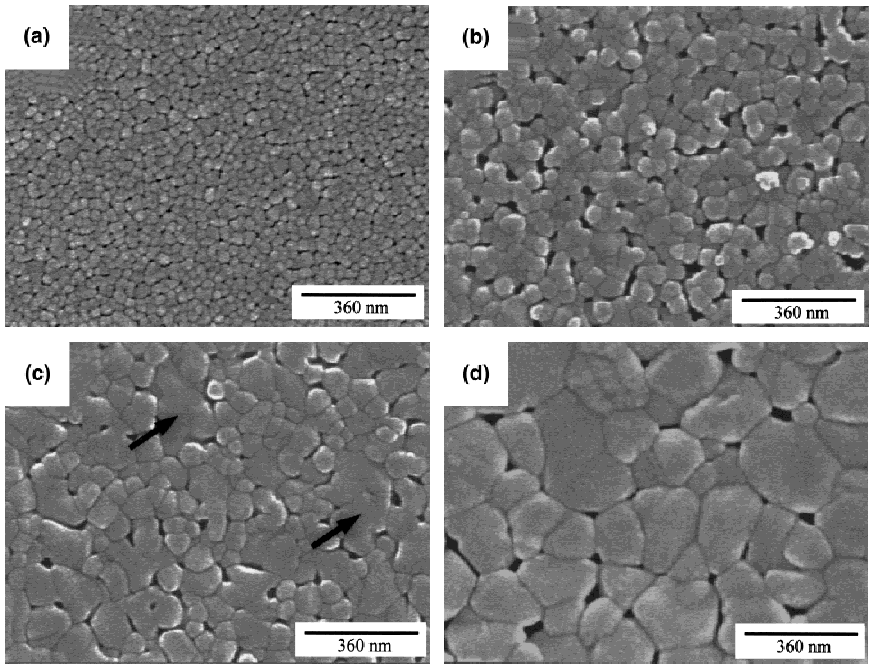

FIG. 6. Microstructural evolution of MOD-TiO_2 films annealed at (a) 700 °C/60 min, (b) 780 °C/30 min, (c) 780 °C/60 min, and (d) 780 °C/90 min.

between the SG- and MOD-TO_2 films will be used to estimate the occurring sequence of A → R phase transformation for the SG- and MOD-TO_2 films. The SSA is estimated by assuming a spherical grain to be 0.22 nm^2/nm^3 for the MOD-TiO_2 films and 0.17 nm^2/nm^3 for the SG-TiO_2 films at 700 °C, suggesting a greater proportion of potential nucleation sites developed in the MOD-TiO_2 films. This may explain a lower transformation temperature observed for the MOD-TiO_2 films; i.e., the phase transformation is accelerated. Additionally, the surface structure may be in a form of –Ti–O · (unpaired oxygen) or –Ti–OH (hydroxyl groups), which are essentially highly active. A higher mobility of surface atoms is expected, which facilitates further coalescence between grains at during the A → R phase transformation situation. This coalescence phenomenon is potentially significant for smaller grains, and an Ostwald ripening mechanism[33] is expected to dominate the grain growth, leading to the formation of porosity [Fig. 6(b)] and bimodal grain size distribution [Fig. 6(d)] for the MOD-TiO_2 films.

The grain size for both films was determined as a function of temperature shown in Fig. 7, where the rapid increase of grain size is observed with sintering temperature after 780 °C for the MOD-TiO_2 film and 930 °C for the SG-TiO_2 film. This behavior could be illustrated by a mechanism termed phase-transformation-induced grain growth.[34] These temperature ranges are approximately equal to that observed for the phase transformation (depicted in Fig. 1). This finding suggests the existence of a critical grain size to the A → R phase transformation

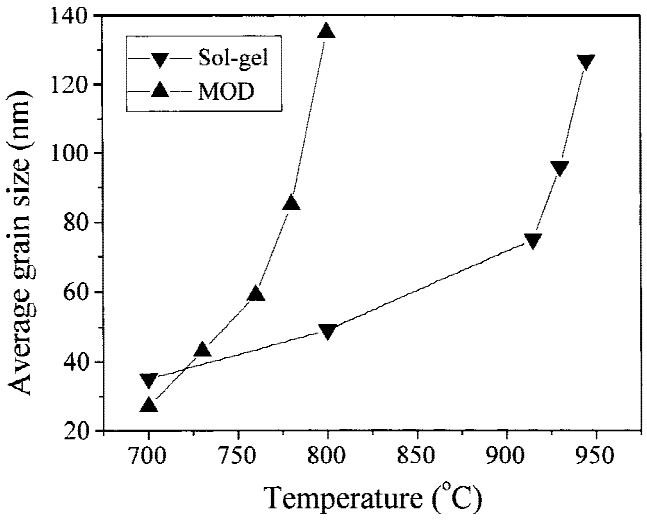

FIG. 7. Dependence of grain size of SG- and MOD-TiO_2 films on different annealing temperatures for 1 h.

for both TiO_2 films. For the SG-TiO_2 films, the critical grain size is about 75 nm and for the MOD-TiO_2 films, it is about 59 nm. We believe that the transformation kinetics of the MOD-TiO_2 films or SG-TiO_2 films is strongly dependent on the critical grain size.

D. Kinetics

From our viewpoint, we believe that the activation energy should be involved to overcome the effects of the substrate constrain and to lead to the amorphous-to-anatase (Am → A) transformation (i.e., crystallization),

rather than being supplied only for the anatase-to-rutile (A → R) phase transformation. A model, which has recently been proposed by Tagami *et al.*[35,36] for phase transformation in a thin layer, was used to characterize the transformation kinetics of both films:

$$\frac{dy}{dt} = Bt^{n-1}(1-y)^{2-\gamma} \quad , \tag{2}$$

where y is the fraction of rutile phase developed at a given time t, k is the reaction rate constant, and B is a model-dependent factor. The n is the time exponent, depending on the mechanism of nucleation/growth of an emerging phase. The explicit value of γ is equal to 15/32 for growing spherical crystallites in three dimensions. After rearrangement and integration, Eq. (2) gives:

$$\frac{1.89}{(1-y)^{0.53}} = (kt)^n \quad , \tag{3}$$

a plot of ln $[1.89/(1-y)^{0.53}]$ versus ln(t) with the slope equal to the exponent n and the intercept equal to ln(k). The activation energy (Q) for the transformation can then be obtained from the slope of a plot of ln(k) versus $1/T$, assuming Arrhenius behavior [$k \propto \exp(-Q/RT)$]. The data presented in Fig. 4 were fit to Eq. (3), and the dependence of k on temperature (in Arrhenius from) is shown in Fig. 8. The Q values were estimated as 524 and 882 kJ/mol for MOD- and SG-TiO_2 films, respectively. We note that the obtained Q values in TiO_2 films are close to those Q (250–853 kJ/mol) reported for TiO_2-based powders,[10,29,37] even though the as-prepared MOD- or SG-TiO_2 films contain substrate constraint and an amorphous phase, which can cause a change in the rate of phase transformation. We also note that the n values obtained for the MOD- and SG-TiO_2 films were 2.9 and 2.1, respectively, indicating diffusion controlled growth, but with different nucleation rates.[38] This result is consistent with our suggestion that a faster rate of nucleation and/or growth can be achieved for the MOD-TiO_2 film.

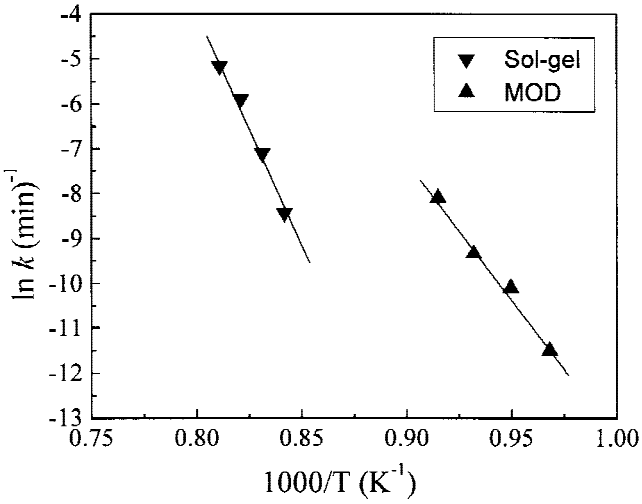

FIG. 8. Relationship of ln k versus $1/T$ for the SG- and MOD-TiO_2 films.

From the kinetic viewpoint, higher activation energy for the phase transformation means that a higher energy barrier needs to be overcome during the reaction. The factors that affect the height of energy barrier should include the effect of substrate constraint, the breaking and rearrangement of Ti–O bonds, and the grain size of untransformed films. If it is assumed that the MOD- and SG-TiO_2 films have the same substrate constraint and the same bond strength to Ti–O, then the major difference in activation energy between MOD- and SG-TiO_2 films is primarily attributed to the grain size. Since the critical grain size in MOD-TiO_2 film is smaller than SG-TiO_2 film, the MOD-TiO_2 film has more surface/grain boundaries nucleation sites to accelerate the A → R reaction. Therefore, MOD-TiO_2 film has a lower phase transformation temperature with smaller activation energy.

IV. CONCLUSIONS

(1) The anatase phase TiO_2 film was completely transformed into single rutile phase in both SG- and MOD-TiO_2 films at 700–1000 °C annealing.

(2) The chemical reactivity of the ligand groups, which are initially coordinated on the titanium precursors, plays a decisive role in structure evolution of SG- and MOD-TiO_2 films.

(3) MOD-TiO_2 films had a higher crystallization temperature than SG-TiO_2 films but the transformation temperature of the anatase-to-rutile TiO_2 phase is much lower in MOD- (approximately 775 °C) as compared to SG-TiO_2 films (approximately 930 °C).

(4) The lower activation energy (524 kJ/mol) in MOD-TiO_2 films, as compared to that (882 kJ/mol) in SG-TiO_2 films is attributed to smaller grain size and more potential nucleation sites existing in the untransformed MOD-TiO_2 film structure.

(5) MOD-TiO_2 films consist of small aggregated particles and therefore tend to coalesce together to form an inhomogeneous microstructure during the A → R transformation. On the other hand, SG-TiO_2 films consist of uniform large particles that tend to grow homogeneously.

ACKNOWLEDGMENTS

The authors would like to thank the National Science Council of the Republic of China, Taiwan, for financially supporting this research under Contract No. NSC-87-2218-E-009-016. Dr. D.M. Liu is appreciated for helpful discussions.

REFERENCES

1. G.P. Burns, J. Appl. Phys. **65,** 2095 (1965).
2. F.B. Hadj, R. Sempere, and J. Phalippou, J. Non-Cryst. Solids **82,** 417 (1986).
3. M.Gratzel, Coments Inorg. Chem. **12,** 93 (1991).
4. G. Yi and M. Sayer, J. Sol-Gel Sci. Technol. **6,** 65 (1996).
5. G. Yi and M. Sayer, J. Sol-Gel Sci. Tech. **6,** 74 (1996).
6. C.J. Brinker and G.W. Scherer, *Sol-Gel Science* (Academic Press, New York, 1990), p. 58.
7. F. Babonneau, S. Doeuff, A. Leaustic, C. Sanchez, C. Cartier, and M. Verdaguer, Inorg. Chem. **27,** 3166 (1988).
8. C. J. Brinker and G.W. Scherer, *Sol-Gel Science* (Academic Press, New York, 1990), p. 46.
9. C.N.R. Rao, S.R. Yoganarasimhan, and P.A. Faeth, Trans. Faraday Soc. **57,** 504 (1961).
10. R.D. Shannon and J.A. Pask, J. Am. Ceram. Soc. **48,** 391(1965).
11. E.E. Yoldas, J. Mater. Sci. **21,** 1087 (1986).
12. S. Doueff, M. Henry, C. Sanchez, and J. Livage, J. Non-Cryst. Solids **89,** 206 (1987).
13. J.F. Quinson, M. Chatelut, C. Guizard, A. Larbot, and L. Cot, J. Non-Cryst. Solids **121**, 72 (1990).
14. Y.J. Kim and L.F. Francis, J. Mater. Sci. **133,** 4423 (1998).
15. M.I. Mendelson, J. Am. Ceram. Soc. **52**, 443 (1969).
16. X.Z. Ding and X.H. Liu, J. Mater. Res. **13,** 2556 (1998).
17. J.D. DeLoach, G. Scarel, and C.R. Aita, J. Appl. Phys. **85,** 2377 (1999).
18. F. Babonneau, A. Leaustic, and J. Livage in *Better Ceramics Through Chemistry III*, edited by C.J. Brinker, D.E. Clark, and D.R. Ulrich (Mater. Res Soc. Symp. Proc. **121**, Pittsburgh, PA, 1988), p. 310.
19. K. Nakamoto, *Infrared and Raman spectra of Inorganic and Coordination Compounds*, 3rd ed. (Wiley, New York, 1978).
20. J. Catterick and P. Thornton, in *Advanced Inorganic Chemistry and Radio Chemistry*, edited by H.J. Emeleus and A.G. Sharpe (Academic Press, New York, London, 1977), Vol. 20, p. 291.
21. K.H. Von Thiele and M. Panse, Z. Anorg. Allg. Chem. **441,** 23 (1978).
22. S. Doeuff, M. Henry, C. Sanchez, and J. Livage, J. Non-Cryst. Solids **89,** 206 (1987).
23. D.C. Eradley, R.C. Mehrotra, and D.P. Gaur, *Metal Alkoxide* (Academic Press, New York, 1978), p. 118.
24. M.L. Calzada and L.D. Olmo, J. Non-Cryst. Solids **121,** 416 (1990).
25. S.B. Amor, G. Baud, J.P. Besse, and M. Jacquet, Mater. Sci. Eng. **B47,** 110 (1997).
26. R. Debnath and J. Chaudhuri, J. Mater. Res. **7,** 3348 (1992).
27. J.A. Gamboa and D.M. Pasquevich, J. Am. Ceram. Soc.**75,** 2934 (1992).
28. R.A. Spurr and H. Myers, Analytical Chemistry **29,** 760 (1957).
29. J.H. Jean and S.C. Lin, J. Mater. Res. **14,** 2922 (1999).
30. R.D. Shannon and J.A. Pask, Am. Mineralogist **49,** 1707 (1964).
31. K.P. Kumar, K. Keizer, and A.J. Burggraaf, J. Mater. Chem. **3,** 917 (1993).
32. A.A. Gribb and J.F. Banfield, Am. Mineralogist **82,** 717 (1997).
33. M. Barsoum, *Fundamentals of Ceramics* (McGraw-Hill, New York, 1997), p. 364.
34. K.P. Kumar, K. Keizer, A.J. Burggraaf, T. Okubo, H. Nagamoto, and S. Morooka, Nature (London) **358,** 48 (1992).
35. T. Tagami and S.I. Tanaka, Acta Mater. **45,** 3341 (1997).
36. T. Tagami and S.I. Tanaka, J. Mater. Sci. **34,** 355 (1999).
37. J. Yang and J.M.F. Ferreira, Mater. Res. Bull. **33,** 389 (1998).
38. J.W. Christian, *The Theory of Transformations in Metals and Alloys* (Pergamon, London, United Kingdom, 1965), p. 525.